KAWASAKI STEEL TECHNICAL REPORT
No.1 (September 1980)

Development of Steels Resistant to Hydrogen Induced Cracking in Wet Hydrogen Sulfide Environment

Yoichi Nakai, Hayao Kurahashi, Toshihiko Emi, Osamu Haida

Synopsis :
Factors influencing the occurrence of Hydrogen Induced Cracking (HIC) in steel plates for linepipe use have been investigated by means of ultrasonic C-scanning of plate specimens preliminarily immersed into synthetic sea water saturated with H2S. The cracks were most frequently observed in the area corresponding to A- and V-segregates of mother ingots, initiating at elongated MnS inclusions and propagating along anomalous structure in which Mn and P were segregated. The rest area was rather in-susceptible to HIC. The occurrence of HIC in the former area was slightly decreased but could not be prevented even by decreasing average S content of the plates as low as 0.001wt%. The addition of copper markedly reduced the rate of hydrogen permeation, but hardly prevented the formation of HIC. Heat treatments to improve the solute segregation in slabs or to make the structure in plates homogeneous helped decreasing the susceptibility to HIC. The treatments, however, were impracticable for commercial control- rolled plates. An effective means to overcome these difficulties has been found by strictly controlling the ratio of effective cerium or calcium to sulfur in the melt (atomic ratio＞1.5) and preventing the reoxidation of the two elements during the teeming of the melt. Resulting plates subjected to controlled rolling have been highly resistant or totally insusceptible to HIC, exhibiting no defect on the C-scanning.

The body can be viewed from the next page.

KAWASAKI STEEL TECHNICAL REPORT No. 1 September 1980

Development of Steels Resistant to Hydrogen Induced Cracking in Wet Hydrogen Sulfide Environment*

Yoichi NAKAI** Hayao KURAHASHI**
Toshihiko EMI** Osamu HAIDA**

Factors influencing the occurrence of Hydrogen Induced Cracking (HIC) in steel plates for linepipe use have been investigated by means of ultrasonic C-scanning of plate specimens preliminarily immersed into synthetic sea water saturated with H_2S.

The cracks were most frequently observed in the area corresponding to A- and V-segregates of mother ingots, initiating at elongated MnS *inclusions and propagating along anomalous structure in which* Mn *and* P *were segregated. The rest area was rather insusceptible to HIC. The occurrence of HIC in the former area was slightly decreased but could not be prevented even by decreasing average* S *content of the plates as low as 0.001 wt%.*

The addition of copper markedly reduced the rate of hydrogen permeation, but hardly prevented the formation of HIC. Heat treatments to improve the solute segregation in slabs or to make the structure in plates homogeneous helped decreasing the susceptibility to HIC. The treatments, however, were impracticable for commercial control-rolled plates.

An effective means to overcome these difficulties has been found by strictly controlling the ratio of effective cerium or calcium to sulfur in the melt (atomic ratio ≥ 1.5*) and preventing the reoxidation of the two elements during the teeming of the melt. Resulting plates subjected to controlled rolling have been highly resistant or totally insusceptible to HIC, exhibiting no defect on the C-scanning.*

1 Introduction

Many accidental defects and failures have been reported on the steel constructions used under wet hydrogen sulfide environment. In general, two types of cracking are observed under the wet hydrogen sulfide environment. The one is the Sulfide Stress Corrosion Cracking[1] (SSCC) which arises from the hydrogen embrittlement[2,3] and the other is the Hydrogen Induced Cracking (HIC) such as the blistering[4].

The former is normally observed in high strength steels under externally or internally stressed or strained condition, and is mainly found in tubings or casing and drilling goods for sour oil well field[5] or in spherical storage tunks for LPG. While, the latter is observed in both high and low strength steels even under nonstressed condition, although mainly found in the low strength steels for gas transmission pipe lines. The Hydrogen Induced Cracking occurs parallel to plate surface, whereas the Sulfide Stress Corrosion Cracking generally develops perpendicular to plate surface or to tensile stress direction.

Despite numerous researches conducted so far on SSCC, only a few are available on HIC[6~10]. Recently many serivce failures[4,11~18] such as oil leakage or bursting due to HIC were reported in the sour gas transmission pipelines. Since then, steel makers have been strongly requested to develop steels which possess sufficient resistance to HIC.

The present investigation is concerned with HIC in linepipe steels and the development of the steel highly resistant to HIC.

*Originally published in Transactions ISIJ, Vol.19 No.7, 1997, pp. 401-410 and rearranged with some modifications
*Research Laboratories

2 Evaluation of Susceptibility to HIC

A laboratory scale method suitable to assess the susceptibility to HIC under wet hydrogen sulfide environment has been developed recently by H. C. Cotton of the British Petroleum Company[19,20]. This test is called "B.P. Test" and is now widely adopted to evaluate the susceptibility to HIC for linepipe steels. The standard test conditions for the B.P. test are shown in **Table 1**. These conditions are considered to correspond to severe service conditions under which linepipes are exposed to sour oil or gas.

In the present investigation, specimens (plate thickness × 100 mm × 100 mm) were cut from commercially produced plates. After pickling by acid for descaling, specimens were immersed into the test solution for 96 hr following the conditions in **Table 1**. All of the hydrogen induced cracks occurring in the specimen were detected by scanning ultrasonic test (C-scanning UST). Then, three coupons were cut from each specimen, and at 3 sections of each coupons (9 sections for 3) sectioned transversely to the rolling direction, the hydrogen induced cracks were examined by microscopy as shown in **Figs. 1** and **2**.

Table 1 Standard condition of B.P. test

Test solution	Synthetic sea water (ASTM D1141-52 stock solution No.1+2)
Temperature	25±3 °C
H_2S concentration	2 300~3 500 ppm saturated condition
pH value	5.1~5.4
Test period	96 hr

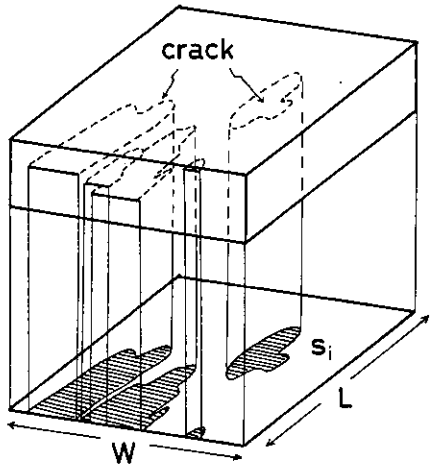

Ratio of crack area by UST

$$= \frac{\text{total projected crack area } (\Sigma s_i)}{\text{area of specimen } (LW)} \times 100\%$$

Fig. 1 Evaluation of cracking susceptibility; ratio of crack area by UST

The susceptibility to HIC was evaluated by three different ways, *i.e.*, (1) Ratio of crack area by UST, (2) Ratio of crack length, (3) Cracking sensitivity ratio, as shown in **Figs. 1, 2** and **3**. In the measurement of the cracking sensitivity ratio, it is necessary to distinguish between the straight cracks and the stepwise cracks. In this work, when one crack is located within the circle with radius of 0.5 mm centered at an end of another crack, as shown in **Fig. 3**, the two cracks are considered to be the components of a stepwise crack.

Among these three evaluations of the susceptibility to HIC, the method by the C-scanning UST gives most reliable measure because C-scanning UST detects all of the cracks in the test specimen. Furthermore, this method has advantage over other two in that the propagation of cracks can be continuously observed by immersing one side of the specimen in the synthetic sea water saturated with hydrogen sulfide and detecting cracks from the other side. An example of such observation is shown in **Fig. 4**.

The relation between the ratio of crack area by UST and the ratio of crack length is shown in **Fig. 5**,

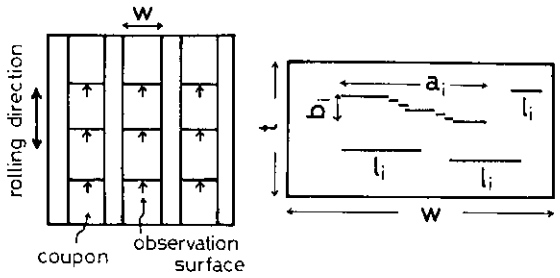

Ratio of crack length

$$= \frac{\text{total crack length } (\Sigma l_i)}{\text{width of sectioned coupon (w)}} \times 100\%$$

Cracking sensitivity ratio

$$= \frac{\text{total stepwise cracking area } (\Sigma a_i b_i)}{\text{cross sectional area of sectioned coupon (wt)}} \times 100\%$$

Fig. 2 Evaluation of cracking susceptibility; ratio of crack length, cracking sensitivity ratio

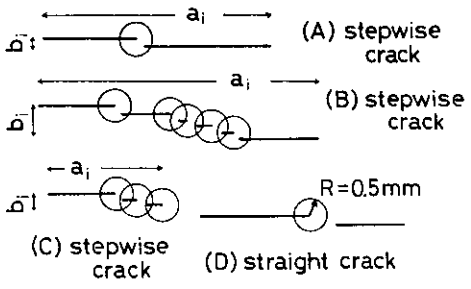

Fig. 3 Method to distinguish between straight crack and stepwise crack

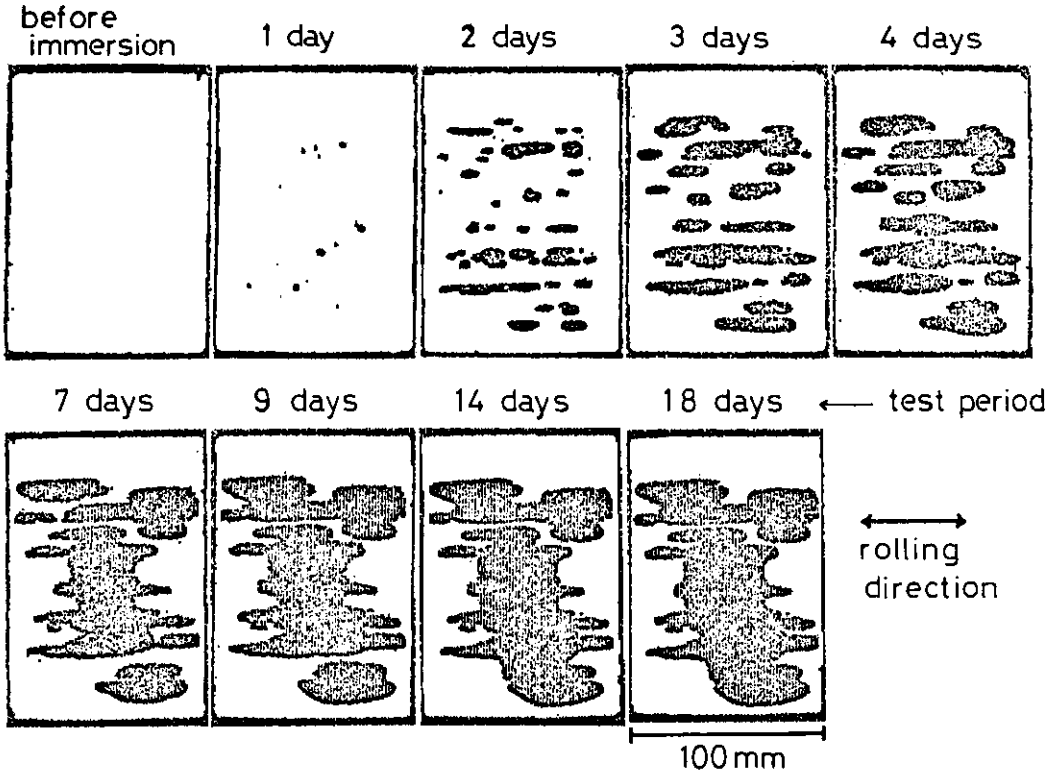

Fig. 4 Propagation of hydrogen induced cracks observed by immersing one side of the specimen in the synthetic sea water saturated with H_2S and detecting cracks from the other side by the C-scanning ultrasonic test

indicating almost one to one correspondence. The relation between the ratio of crack area by UST and the cracking sensitivity ratio is shown in **Fig. 6**. The cracking sensitivity ratio is approximately zero when the ratio of crack area by UST is less than 20 %. Hence, this value of 20 % can be regarded as the critical value whether the stepwise cracks occur or not in the pipeline steel used under the wet hydrogen sulfide environment. If the bursting of the pipe is considered to occur mainly when linking of the stepwise

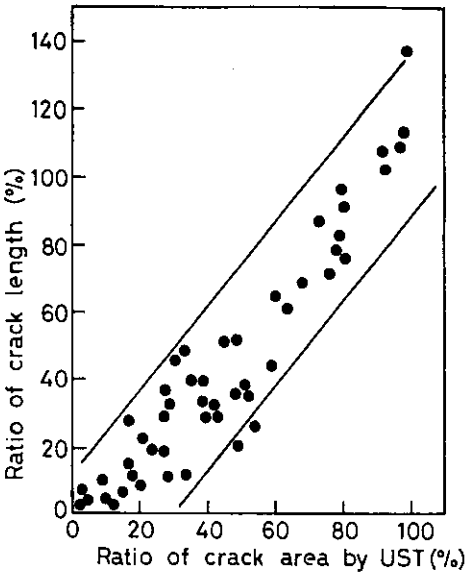

Fig. 5 Relation between ratio of crack length and ratio of crack area by UST

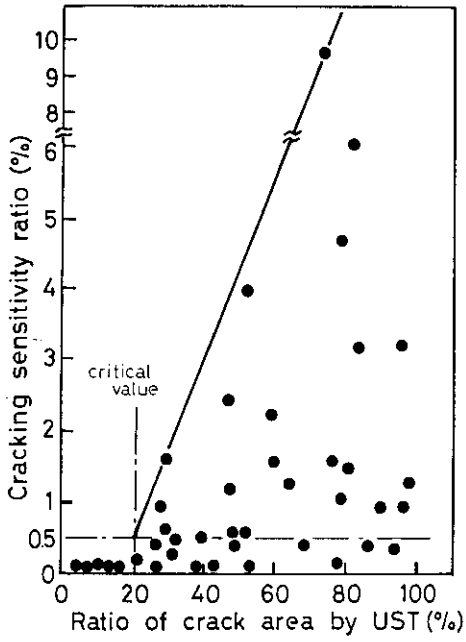

Fig. 6 Relation between cracking sensitivity ratio and ratio of crack area by UST

crack in through-thickness direction is developed, the steel of which the ratio of crack area by UST is less than 20 % can be considered to be the steel highly resistant to HIC.

In evaluating the susceptibility to HIC for steels of commercial scale production, it is found to be very important to specify the sampling position of the specimens because the susceptibility to HIC depends largely upon the distribution of the segregation such as A- and V-segregates in ingots. An example of the change of the susceptibility to HIC with the position in mother ingot is shown in **Fig. 7**. The specimens corresponding to the center of the width at the top or the middle portion of the height of the ingot have higher susceptibility to HIC compared with the specimens corresponding to the edge or the bottom of the ingot. Thus, in the present investigation, specimens cut from the high susceptible location within plates were used to compare various processes to improve the susceptibility to HIC of steels.

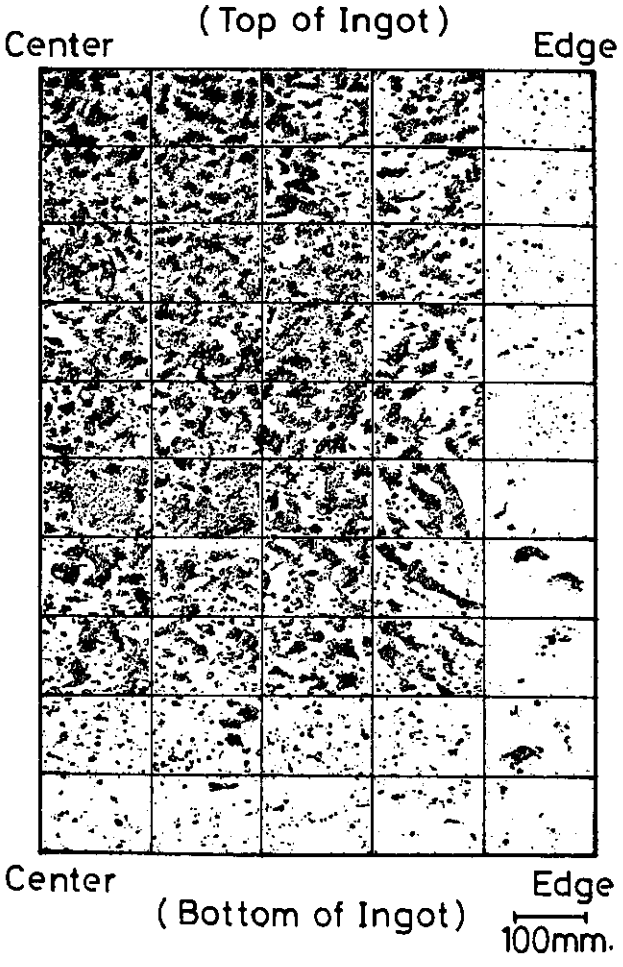

Fig. 7 Change of the susceptibility to HIC with the position in mother ingot

3 Metallographic Examination

The typical blisters observed on the surface of the specimen subjected to the B.P. test shown in **Table 1** are shown in **Photo. 1**. The cross sectional view shows that the blistering is caused by the cracks near the surface and most of these cracks are stepwisely continued to the surface. Further microscopic study revealed that the occurrence of the blistering depends on the number and size of inclusions but not on their types.

It should be noted, however, that there are often observed internal cracks when the blisters are not observed and such internal cracks are much more detrimental for the accidental defects and failures of the pipelines as will be shown later. These internal cracks can be classified into two types as shown in **Photo. 2**, the straight crack parallel to the plane of rolling and the stepwise crack which consists of cracks on different planes linked thicknesswise by small cracks. Normally, both types of internal cracks are observed simultaneously. The crack openings (displacement values) range up to approximately 10 μm, resulting in large localized deformation near the ends of the straight cracks and around the smaller stepwise cracks.

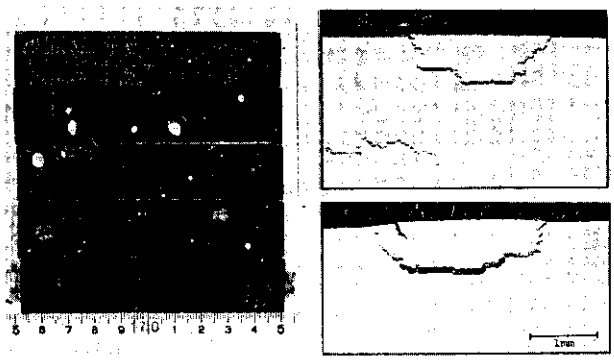

Photo. 1 Typical blisters observed on the surfaces and in the cross sections of the specimens subjected to the B.P. test

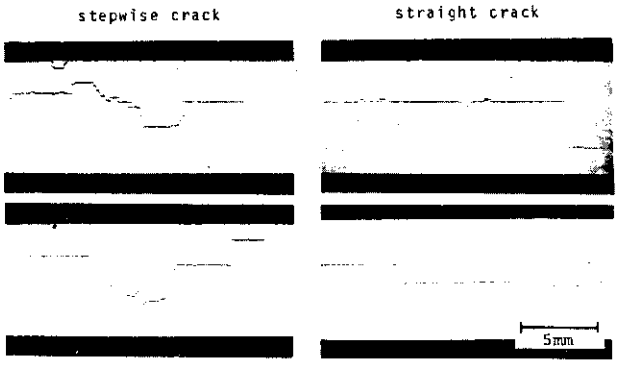

Photo. 2 Typical hydrogen induced cracks observed in the specimens subjected to the B.P. test

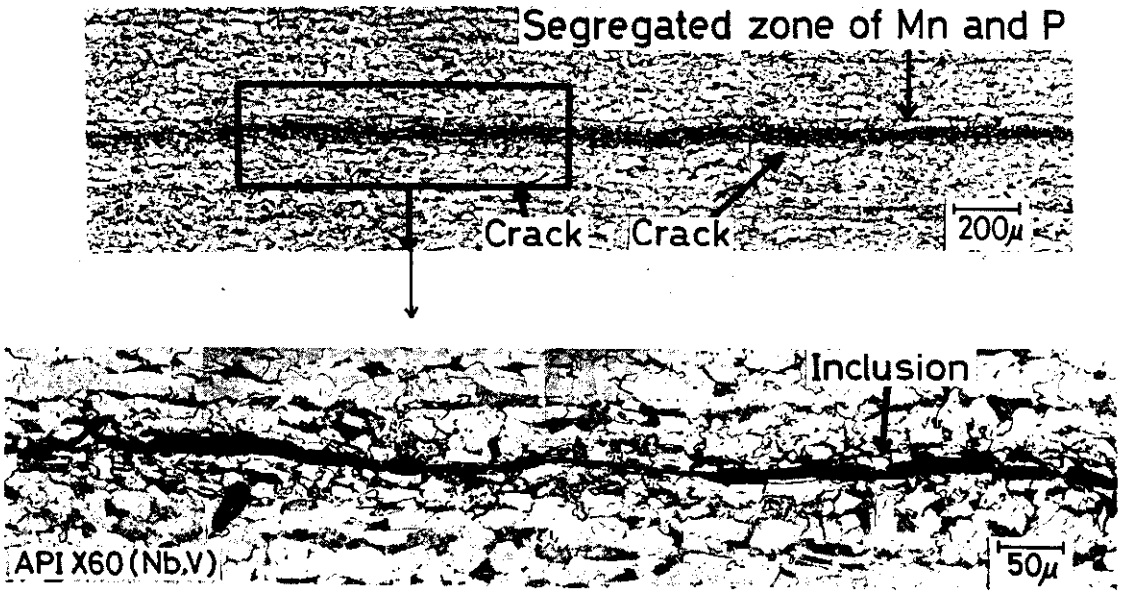

Photo. 3 Optical micrograph of the micro-structure around the cracks etched by picric acid solution containing surfactant

Optical micrograph of the microstructure around the cracks etched by picric acid solution containing surfactant is shown in **Photo. 3**. Cracks are found in the strongly etched band structure and always accompanied by type *II* nonmetallic inclusions. The X-ray microprobe line analysis across the crack given in **Fig. 8** clearly shows the positive segregation of Mn and P around the crack and high peaks of Mn and S in the crack. The qualitative analysis of the inclusions associated with the crack revealed that the inclusion was type *II* MnS. The segregated zone of Mn and P in **Fig. 8** corresponds to the strongly etched band structure in **Photo. 3**. These observations clearly show that the initiation site of the cracks is type *II* MnS inclusion in the band structure.

In addition, the straight cracks parallel to the plane of rolling are generally propagated, as shown in **Photo. 3**, along the pearlite bands or the bainitic or martensitic structure found in the segregation zone of Mn and P. The bainitic or martensitic structure is apt to

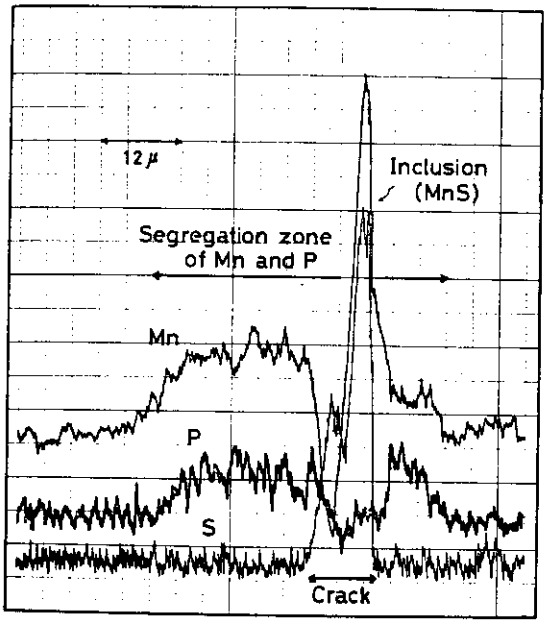

Fig. 8 E.P.M.A. analysis for the segregated zone of Mn and P corresponding to strongly etched band structure in **Photo. 3**

Photo. 4 Scanning electron micrograph of the fractured surface of the straight crack

occur in the segregation zone of Mn and P during the cooling of plates after hot rolling.

The scanning electron micrograph of the fractured surface of the straight crack, as shown in **Photo. 4**, shows that the fracture is sub-cleavage configuration, the same as the hydrogen embrittlement fracture in steels.

As described before, there are three types of crack, *i.e.*, blister, straight crack and stepwise crack. Some researchers[19,20] claim that only the stepwise crack is dangerous assuming that the bursting occurs when linking of the cracks in through thickness direction is developed. The following result, however, shows that not only the stepwise crack but also the large straight crack is dangerous for the bursting of pipe. In the sample cut from a linepipe (API 5LS X42, 24″ × 0.25″, S = 0.026 wt%) used for sour gas service that actually burst during the operation, many large straight cracks are observed near the fractured part of the pipe as shown in **Photo. 5**. The scanning electron micrograph of the fractured surface of this straight crack revealed that there were large clusters of type *II* MnS inclusions in accordance with the foregoing result for laboratory research.

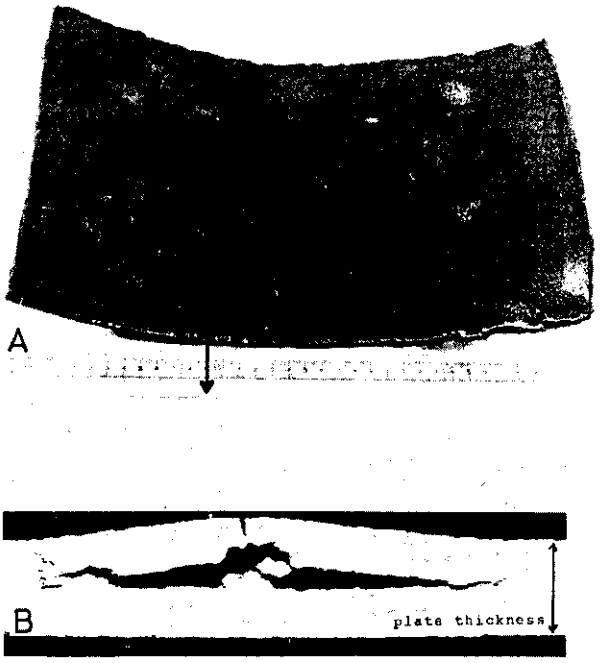

Photo. 5 Hydrogen induced cracks observed on the inner wall of the linepipe used for sour gas service that actually burst during the operation

4 Improvement of Resistance to HIC

Taking account of the metallurgical factors for HIC, described in the foregoing paragraph, several measures to improve the resistance of steel to HIC can be considered, as shown in **Fig. 9**. These measures can be classified into the following three groups:

(1) The measure to reduce the amount of entrance of hydrogen into steel,
(2) The measure to reduce the number of crack initiation sites, and
(3) The measure to prevent crack propagation.

Results of the laboratory and commercial scale

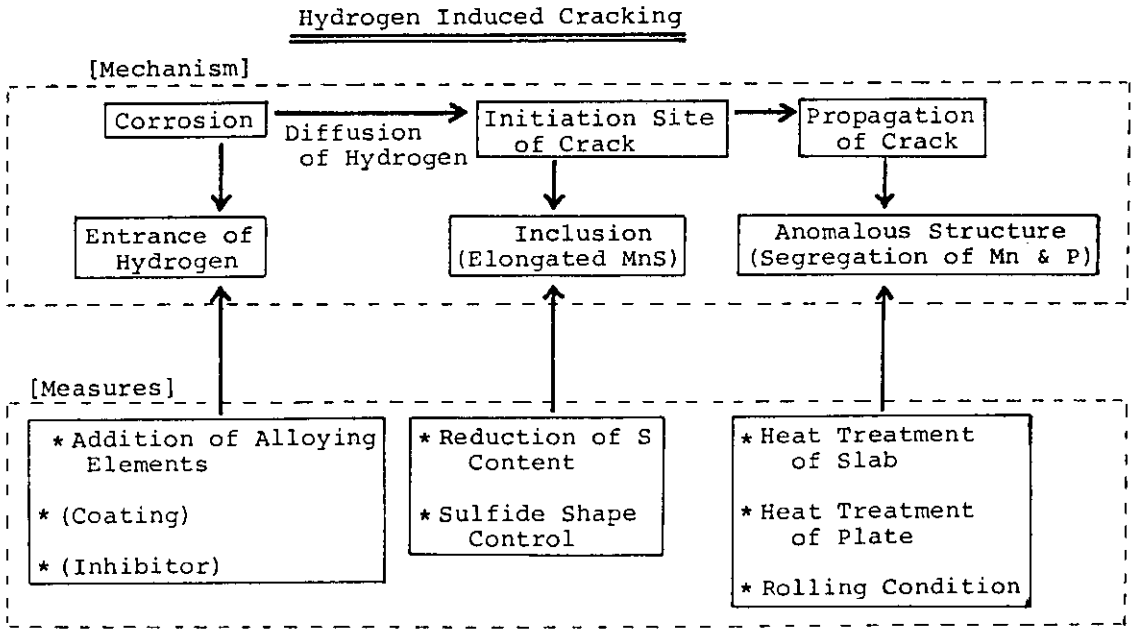

Fig. 9 Mechanism of HIC and measures to improve the resistance of steel to HIC

examinations to improve the resistance to HIC will be described in this section.

4.1 Effect of Alloying Elements on Entrance of Hydrogen into Steel

Since HIC is caused by hydrogen entering into steels from their surface, reduction in the amount of entrance of hydrogen into steels under wet hydrogen sulfide environment is expected to restrain the occurrence of HIC. The amount of hydrogen entering into steels can be determined most effectively and accurately by electrochemical measurement[21,22] of the rate of hydrogen permeation. One side of the surface of the specimen is exposed to H_2S-saturated synthetic sea water, and the amount of the hydrogen permeation is measured as the anodic current. A typical result of the measurement is shown in **Fig. 10**. The current for hydrogen permeation increases to a maximum value (J_{max}) after a few hours and then decreases to steady state value (J_∞) after a few ten hours as the film of corrosion product becomes stable.

Fig. 11 shows the effect of the alloying elements on the hydrogen permeation rate for the steels which were prepared by melting electrolytic iron and adding alloying elements under vacuum in an induction furnace of 30 kg capacity. The hydrogen permeation current (J_∞) is clearly decreased with increasing content of Cu in electrolytic iron. The effect of Cu for 0.17C–0.25Si–1.45Mn–0.018Nb–0.020Al steels were

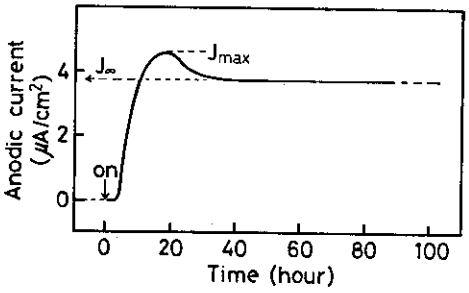

Fig. 10 Typical permeation curve

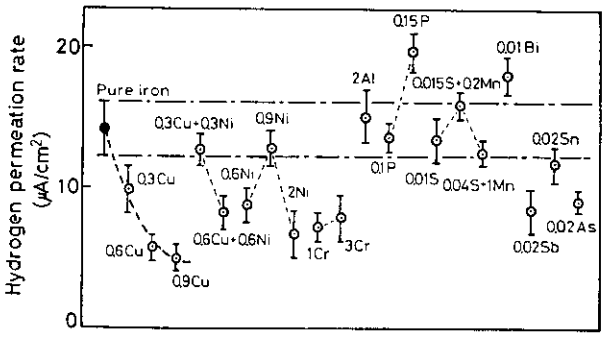

Fig. 11 Effect of alloying elements of hydrogen permeation rate for the steels prepared by melting electrolytic iron

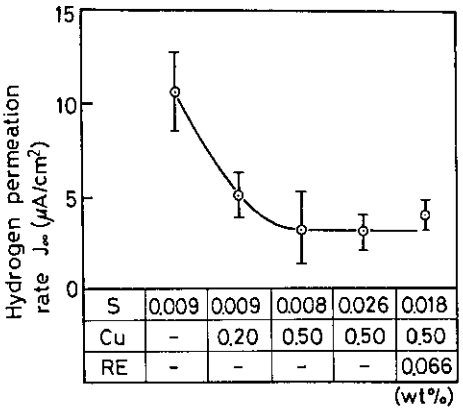

Fig. 12 Effect of Cu content on hydrogen permeation rate for the laboratory-melted steels (0.17C–0.25Si–1.45Mn–0.018Nb–0.020Al)

also examined with laboratory-melted specimens, and is shown in **Fig. 12**. The hydrogen permeation rate markedly decreases to less than one-half of the initial value with Cu of 0.2% or more. Mechanism for such remarkable decrease is not fully understood for the present, but it is probable that Cu inhibits the surface corrosion reaction hence diminishes the entrance of hydrogen from environment into steel matrix.

4.2 Effect of Sulfur Content on Susceptibility to HIC

As already described above, inclusions, particularly manganese sulfides, have trigger effect for the crack formation. Consequently, reduction of S content has been thought to be an effective way to decrease the susceptibility to HIC[20].

The effect of S content on HIC was examined first in laboratory scale experiment. Ingots prepared by the vacuum melting were forged to slabs of 80 mm in thickness which were rolled into plates of 11.5 mm in thickness under three different rolling conditions.

The susceptibility to HIC of these plates was rated in terms of the ratio of crack length, the result being given in **Fig. 13**. The ratio of crack length decreased,

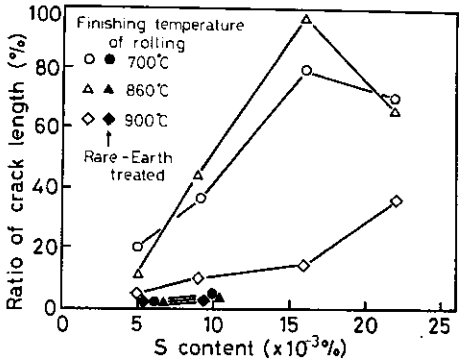

Fig. 13 Effect of S content on HIC for the laboratory-melted steels (0.10C–0.25Si–1.40Mn–0.040Nb–0.023Al)

especially for the control rolled plates markedly with decreasing S content.

Since commercial scale production of steels with S of less than 0.010 % has become quite easy, the susceptibility to HIC of commercial hot-rolled plates containing sulfur of less than 0.006 % was examined. The plates were finished in the temperature range between 700° and 800°C in controlled rolling process. The C and Mn contents of these plates are 0.05 to 0.18 % and 0.75 to 1.90 %, respectively. For other alloying elements such as Nb, V, Ni, Cu, Cr, *etc.*, contents for API 5LB X52 to API 5LX X70 grades were resumed.

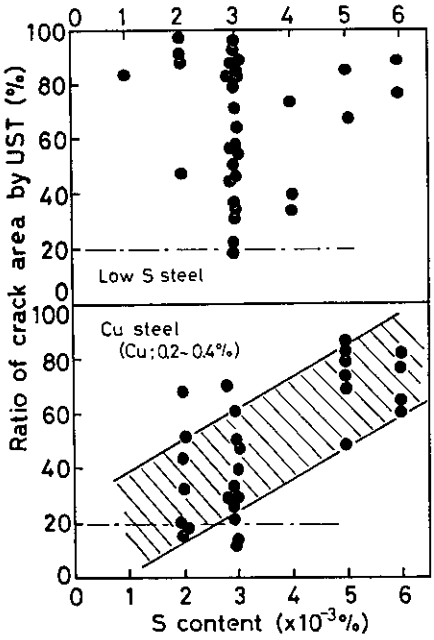

Fig. 14 Effect of S content on HIC at high susceptible location for API 5LX X-52 ~ X70 grade steels

Fig. 14 shows the relationship between the susceptibility to HIC and S content, where specimens were taken from positions corresponding to A- and V-segregates of mother ingots. The HIC susceptibility measured in terms of the ratio of crack area by UST does not depend on the S content if Cu is not contained, whereas it decreased with decreasing S content for Cu containing steels. However, the HIC cannot be completely prevented in the segregates region even if Cu is added and S content is decreased as low as 0.002 %, indicating that in the segregates region many MnS inclusions are still remained to initiate cracks.

4.3 Effect of Shape Control of Nonmetallic Inclusions on Susceptibility to HIC

It is well known that the deoxidation condition affects the morphology of MnS inclusions[23,24], *i.e.*, in steels with rather high free oxygen concentration, such as semi-killed and Si-killed steels, type *I* MnS is predominant which has higher resistance to the deformation during hot rolling than type *II* MnS predominant in Al-killed steels.

The effect of type of MnS on the susceptibility to HIC is compared between semi-killed and Al-killed steels. Specimens for this purpose were prepared by rolling in the laboratories small slabs cut from commercially produced slabs including A- and V-segregates of mother ingots.

Steel	Al-killed steel	Si-Al-killed steel	Semi-killed steel
C	0.12	0.17	0.18
Si	0.27	0.26	0.028
Mn	1.41	1.23	0.85
S	0.005	0.011	0.020
Cu	0.25	—	—
Ni	0.18	—	—
Cr	—	0.15	—
Mo	—	0.041	—
Nb	0.036	—	—
Al	0.035	0.008	—
Inclusion	II-type MnS, Al_2O_3	II-type MnS, Al_2O_3	I-type MnS, Silicates

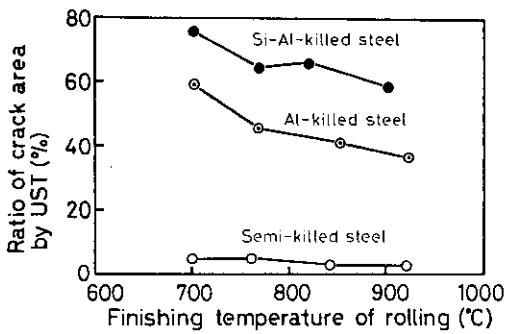

Fig. 15 Comparison of the susceptibility to HIC between semi-killed, Si-Al-killed, and Al-killed steels

The result of this examination is shown in **Fig. 15.** The incidence of cracking was either nil or low in the semi-killed steels where the sulfides remained rather unchanged (ellipsoidal) even if controlled rolling was adopted. On the contrary, cracking was prevalent in the fully Al-killed steels, in which the sulfides were deformed into elongated stringer type. The susceptibility to HIC for the fully Al-killed steels increased with the decrease of finishing temperature of rolling.

In spite of the favourable effect to prevent HIC, the shape control of inclusions by the weak deoxidation is often unacceptable because of the requirement for

mechanical properties.

On the other hand, the addition of small amount of rare earths (RE) is known to be useful to spheroidize sulfide inclusions in hot-rolled fully Al-killed steels.

Fig. 13 shows the crack susceptibility of rare earth treated steels prepared by vacuum melting in the laboratories. Unlike non-treated steels, the susceptibility to HIC was either nil or low in the rare earth treated steels even if the controlled rolling was carried out.

The application of this laboratory scale study to the commercial scale production will be described later.

4.4 Effect of Heat Treatment on Susceptibility to HIC

Heat treatment to reduce solute segregation in slabs was expected to make the structure in corresponding plates homogeneous, hence serve to decrease the susceptibility to HIC.

Thus, small slabs were cut from commercially produced, API 5LX X52 quality slab including A- and V-segregates of ingot, heated at 1 250 °C for 0.5 to 24 hr in argon gas, then control-rolled in the same laboratory-rolling condition as mentioned before.

Solute segregation (Mn, P) as represented by the average of maximum peak values measured by EPMA analysis decreased with increasing heating time, but the anomalous structure still remained in the segregates area in plates even after 24 hr of heating. The heat treatment reduces solute segregation to some extent, but does not completely dissolve or transform type *II* MnS, hence incapable of totally prevent HIC as shown in **Fig. 16**.

The effect of normalizing or quench-tempering of the plate on the susceptibility to HIC is also shown in

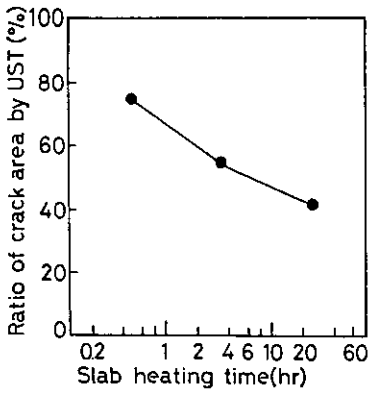

Fig. 16 Effect of slab-heating time on HIC; small slab were cut from commercially produced slab including A- and V-segregates of ingot, heated at 1 250 °C, then control-rolled in laboratory. (0.12C–0.26Si–1.33Mn–0.008S–0.013Nb–0.034Al)

Fig. 17. The two treatments are as well effective to reduce the susceptibility to HIC, the quench-tempering being more effective than the normalizing. However, these heat treatments are not always practicable, since aimed mechanical properties of control-rolled plates will be changed by these treatments.

4.5 Effect of Rolling Condition on Susceptibility to HIC

Plastic deformation of MnS inclusions has been known in conformity with that of steel matrix at 700° to 1 000 °C, whereas it becomes less than that of the matrix above 1 000 °C[25~27]. As a measure of the deformation temperature, finisher departing temperature (FDT) of plates and strips was taken and the

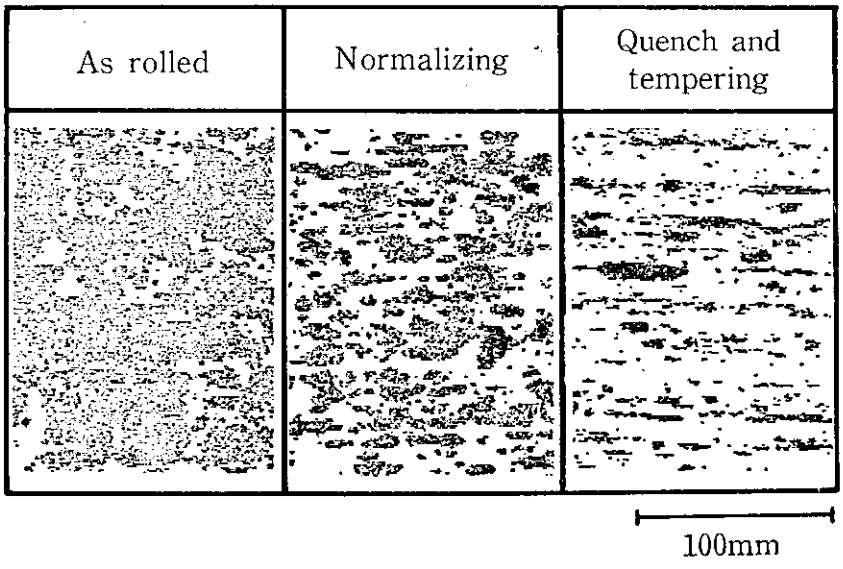

Fig. 17 Effect of normalizing and quench-tempering of plate on HIC for commercial steel

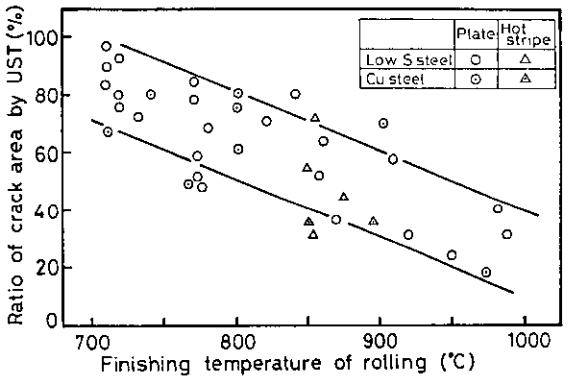

Fig. 18 Effect of final rolling temperature on HIC for commercial hot-rolled plates and strips (0.05–0.14C, 0.21–0.33Si, 0.80–1.45Mn, 0.015–0.023P, 0.003–0.008S, 0–0.065Nb, 0–0.039V, 0–0.31Cu, 0–0.28Ni, 0.025–0.050Al)

effect of the FDT on the susceptibility to HIC was determined in **Fig. 18**. Decreasing finishing temperature clearly increases the susceptibility to HIC, qualitatively reflecting more plastic deformation of MnS at lower temperatures.

5 Development of Steels Insensitive to HIC in Wet Hydrogen Sulfide Environment

In order to establish suitable conditions with which the sulfide shape control becomes complete throughout the ingots, the solute segregation, constitution and distribution of sulfides in many RE- or Ca-treated ingots have been investigated as a function of the concentrations of RE, Ca, S and O in HSLA steel melts.

The melts blown in a 200 t LD converter were deoxidized with Si and Al, alloyed, RH-stirred to remove oxide inclusions to less than 35 ppm of total oxygen content, then teemed into 23 or 26 t ingot molds. RE was added in the ladle and Ca was added from the teeming spout by iron-clad Ca or Ca–Al wire during buttom pouring. The content of Ca and RE was between 0.0024 to 0.0081 % and 0.010 to 0.036 %, respectively.

The bottom cone sedimentation of clustered sulfides and oxy-sulfides has been found to occur at $[\%Ca]\cdot[\%S]^{0.28} \geqq 1 \times 10^{-3}$ in Ca-treated ingots and at $[\%RE]\cdot[\%S] \geqq 1 \times 10^{-4}$ in RE-treated ingots[28~30], as shown in **Fig. 19**. The sedimentation is found detrimental on mechanical properties and resistance to HIC of the steel material. Thus, concentrations of Ca, RE and S in the melt in mould must resume the above criteria to prevent the harmful accumulation of clustered inclusions in the bottom of ingots.

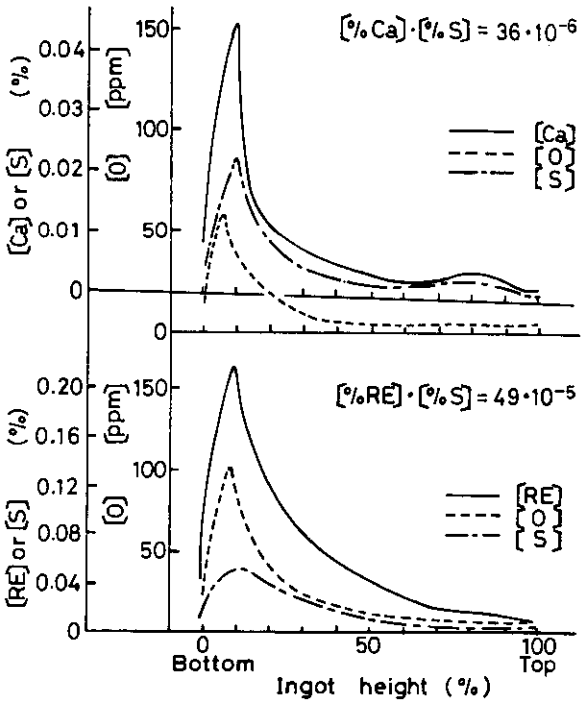

Fig. 19 Distribution of Ca, RE, O, S along the central vertical axis of the ingots which have bottom cone sedimentation of clustered sulfides and oxy-sulfides

The degree of sulfide shape control with Ca or RE has been found to be evaluated favourably in terms of atomic concentration ratio, ACR, of effective Ca or RE to S in the melt in mould[29,30]:

$$ACR_{Ca} = \frac{1}{1.25}\frac{[\%Ca_{eff}]}{[\%S]} \quad \cdots\cdots\cdots\cdots (1)$$

$$ACR_{RE} = \frac{1}{4.38}\frac{[\%RE_{eff}]}{[\%S]} \quad \cdots\cdots\cdots\cdots (2)$$

The concentration of effective Ca, $[\%Ca_{eff}]$, or RE, $[\%RE_{eff}]$, is given by

$$[\%Ca_{eff}] = [\%Ca_{total}]\cdot\{1 - 98[\%O_{total}]\} \cdots (3)$$

$$[\%RE_{eff}] = [\%RE_{total}] - 0.008\ \%$$
$$(O_{total} = 20 \sim 36\ ppm) \cdots\cdots\cdots\cdots (4)$$

which is the difference between the concentration of total Ca or RE and that consumed by reducing oxides such as Al_2O_3 suspending in the melts, *i.e.*, the concentration effective to react with S in the melts. The details of the derivation of Eqs. (3) and (4) are given elsewhere[30].

Careful microscopic measurement of the amount of elongated inclusions in the specimens taken from various part of slabs revealed that the sulfide shape control is incomplete throughout ingots at ACR of 0.2,

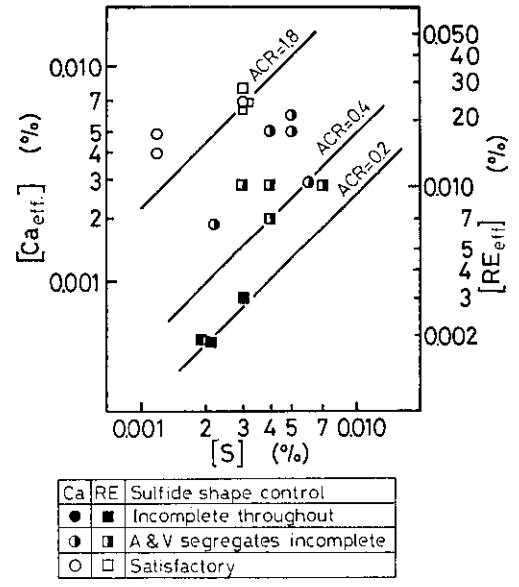

Fig. 20 Influence of the effective concentration and ACR on sulfide shape control

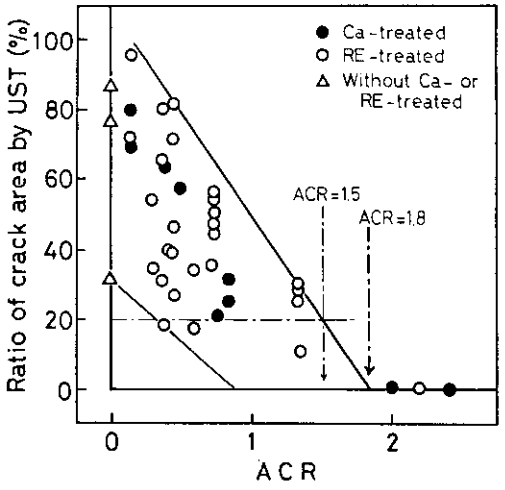

Fig. 21 Effect of the atomic concentration ratio (ACR) of Ca and RE on HIC

satisfactory at 0.4 except for A- and V-segregates, then becomes complete even in the segregates at 1.8 as shown in **Fig. 20**. Thus, the condition required to complete sulfide shape control even in the A- and V-segregates is found for the first time by this work.

On the other hand, the susceptibility to HIC of many commercially produced Ca- or RE-treated plates were examined which were rolled under almost identical controlled conditions. The relationship between the susceptibility to HIC and ACR for the segregates region is shown in **Fig. 21**. The susceptibility to HIC decreases with increasing ACR value. When ACR is above 1.5 the ratio of crack area by UST is less than 20 %. The plate for which this ratio is less than 20 % can be considered highly resistant to HIC, as discussed in *Chapter* **2**. Furthermore, when ACR is above 1.8, plates are totally free from HIC irrespective of the choice of Ca or RE in accordance with the complete shape control as shown in **Fig. 20**. Simple mathematics using eqs. **(1)** and **(3)** shows that ACR values of 1.5 and 1.8 correspond to Ca/S of 1.7 and 3.1, respectively, at O_{total} of 0.0025 %. Thus, by controlling the concentration of Ca or RE and S to fall within the area bound by $[\%Ca_{total}]/[\%S] \geqq 1.7$ (desirably $\geqq 3.1$) and $[\%Ca]\cdot[\%S]^{0.28} < 1 \times 10^{-3}$ or $[\%RE]\cdot[\%S] < 1 \times 10^{-4}$ on Ca or RE *vs.* S coordinates, steels that are highly resistant to HIC have been produced for sour gas service. These steels are named "HIC Free Steel" and can be manufactured on commercial scale. The occurrence of HIC after the B.P. test is compared between the sulfide shape controlled HIC Free Steel and non-shape controlled version in **Fig. 22**. Remarkable decrease in the occurrence of HIC is observed in the HIC Free Steel, in particular, when ACR is above 1.8.

The mechanical properties of the UOE pipe of API 5LX X65 grade made from the HIC Free Steel are compared in **Figs. 23** and **24** with non-shape controlled version. **Fig. 23** shows the result of the tensile

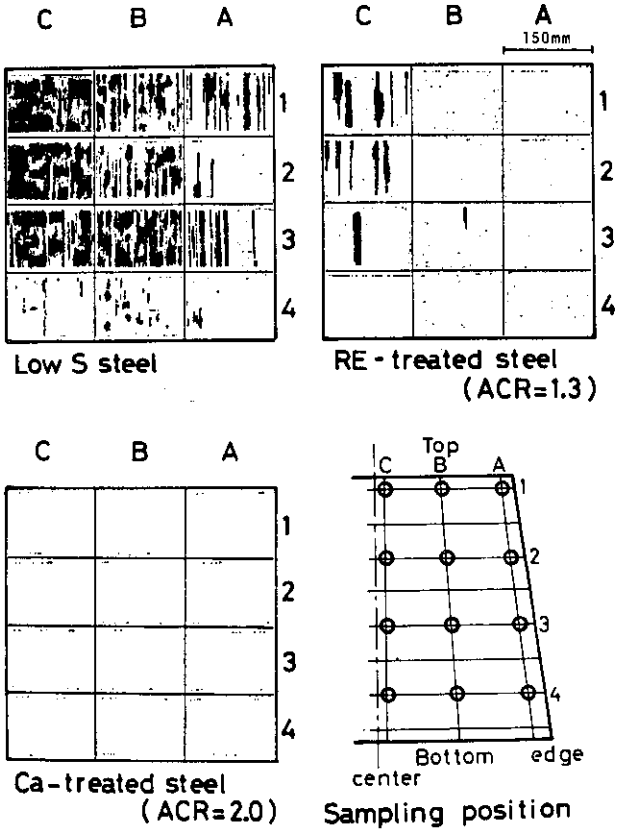

Fig. 22 Comparison of the susceptibility to HIC between low S steel and RE- or Ca-treated steel

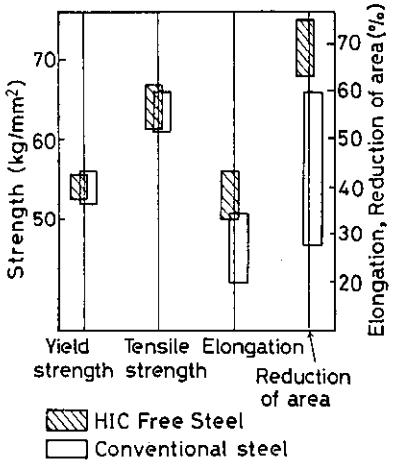

HIC Free Steel (0.10–0.12C, 0.25–0.28Si, 1.25–1.35Mn, 0.014–0.019P, 0.002–0.003S, 0.024–0.040Nb, 0.024–0.035V, 0–0.25Cu, 0.025–0.035Al, 0.0045–0.0073Ca.)
Conventional Steel (0.10–0.13C, 0.23–0.28Si, 1.30–1.45Mn, 0.014–0.020P, 0.003–0.008S, 0.026–0.034Nb, 0.026–0.034V, 0.025–0.035Al.)

Fig. 23 Tensile properties in through-thickness direction for UOE pipe of API 5LX X65 grade

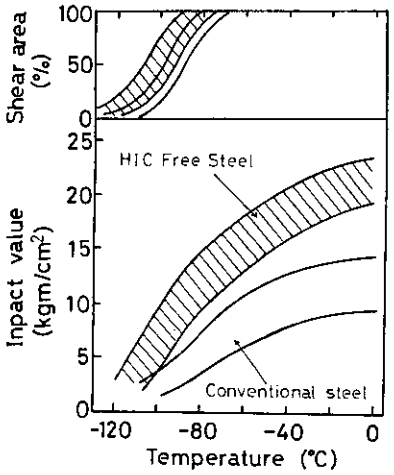

Fig. 24 Charpy 2 mm V-notch transition curves in transverse direction for UOE pipes of API 5LX X65 grade

test in through thickness (Z) direction, indicating that the HIC Free Steel pipe has almost the same strength as the non-shape controlled version, but is far better in elongation and in reduction in area. Result of the Charpy test on 2 mm V-notch specimens taken from the pipe in a direction perpendicular to the weld seam is shown in **Fig. 24**, indicating that the absorbed energy and the transition temperature of the HIC Free Steel pipe is much better than the non-shape controlled pipe. Furthermore, it is confirmed that the HIC Free Steel pipe has almost the same of slightly better properties than the conventional version in the DWTT test and field weldability test.

The pipes made from the HIC Free Steels are suitable for the service in wet hydrogen sulfide environment.

6 Conclusion

(1) The hydrogen induced cracking is most frequently observed in the area corresponding to A- and V-segregates of mother ingots, initiating at elongated MnS inclusions and propagating along anomalous structure in which Mn and P are segregated.

(2) The occurrence of HIC in the segregates locations is slightly decreased but not prevented by decreasing average S content of the plates as low as 0.001 wt%.

(3) The addition of Cu markedly reduces the rate of hydrogen permeation, but hardly prevents the formation of HIC.

(4) The heat treatment to improve the solute segregation in slabs or to make the structure in plates homogeneous helps decreasing the susceptibility to HIC, but the treatment is inapplicable to commercial production of control-rolled plates.

(5) The shape control of inclusions by making deoxidation weaker markedly reduces the formation of HIC, but this is inapplicable to the commercial production of pipes used under severe conditions in view of mechanical properties.

(6) An effective means to overcome these difficulties is found to strictly controlling the ratio of effective RE or Ca to S in the melt (atomic ratio $\geqq$ 1.5) and preventing the reoxidation of the two elements during the teeming of the melt. Resulting plates which subjected to controlled rolling are highly resistant or totally insusceptible to HIC.

From the results of this investigation, the steel highly resistant to HIC in the wet hydrogen sulfide environment has been developed, and named "HIC Free Steel".

References

1) "NACE Technical Practices Committee (1-G) Report", Corrosion, **8** (1952), p. 351.
2) E. Snape: Corrosion, **23** (1967) 6, p. 154
3) R.S. Treseder: Preprint of International Conference of Stress Corrosion Cracking and Hydrogen Embrittlement, NACE, Paris, (1973), No. A-6

4) T. Skei, A. Wachter, W.A. Bonner and H.D. Brunham: Corrosion, **9** (1953), p. 163
5) W. Dahl, H. Stoffels, H. Hengstenberg and C. Duren: Stahl u. Eisen, **87** (1967) 3, p. 125
6) T. Murata, K. Yukawa, H. Tamura, E. Satoo and H. Okada: Tetsu-to-Hagané, **6** (1975) 4, S235
7) A. Ikeda, S. Okamoto, S. Nagata, F. Terasaki and M. Kowaka: Tetsu-to-Hagané, **61** (1975) 4, S237
8) A. Ikeda, S. Nagata, F. Terasaki and E. Miyoshi: Tetsu-to-Hagané, **61** (1975) 4, S238
9) M. Tanimura and T. Nishimura: Tetsu-to-Hagané, **61** (1975) 4, S241
10) M. Tanimura, I. Matsushima, H. Inagaki and T. Nishimura: Tetsu-to-Hagané, **62** (1976) 4, S247
11) I. Class: Proceeding of the 2nd International Congress on Metallic Corrosion, NACE, Houston, (1966), p. 342
12) P.L. Autonce, G. Casarimi and W. Dumini: International Congress of Hydrogen in Metals, ASM, Paris, (1974), p. 520
13) R.R. Irving: Iron Age, **217** (1974) 24, p. 8
14) H. Ishiguro and H. Nishimura: Symposium for Heavy Oil Desulphurization Apparatus, Japan Petroleum Institute, Tokyo, (1973) 25
15) K. Izumi and H. Inagaki: Examples of Corrosion Failures in Petroleum Industries, Japan Petroleum Inst., Tokyo, (1972), p. 119
16) K. Nishimura: Examples of Corrosion Failures in Petroleum Industries, Japan Petroleum Inst., Tokyo, (1972), p. 33
17) F. Paredes and W.W. Mize: Oil & Gas J., **52** (1954), p. 99
18) F.K. Naumann and F. Spies: Praktische Metallographic, **10** (1973), p. 475
19) E.M. Moore and J.J. Warga: "Factors Influencing the Hydrogen Cracking Sensitivity of Pipeline Steels." Preprint of NACE Corrosion '76, Houston, March, (1976), Paper No. 144
20) E. Miyoshi, T. Tanaka, F. Terasaki and A. Ikeda: "Hydrogen Induced Cracking of Steels Under Wet Hydrogen Sulfide Environment", Preprint of the 30th Annual Meeting, A.S.M.E., Oklahoma, September, (1975).
21) J. O'M Bockris, J. McBreen and L. Nanis: J. Electrochem. Soc., **112** (1965), p. 1025
22) J. McBreen, L. Nanis and W. Beck: J. Electrochem. Soc. **113** (1966), p. 1218
23) C.E. Sims: Trans. Met. Soc. AIME, **215** (1959), p. 367
24) T.J. Baker and J.A. Charles: JISI, **210** (1972), p. 702
25) T.J. Baker and J.A. Charles: JISI, **210** (1972), p. 680
26) T.J. Baker and J.A. Charles: JISI, **211** (1973), p. 187
27) P.J. Maunder and J.A. Charles: JISI, **206** (1968), p. 705
28) T. Sakuraya, T. Emi, Y. Habu, A. Ejima and K. Sanbongi: Tetsu-to-Hagané, **62** (1976) 13, p. 1653
29) T. Emi, O. Haida, T. Sakuraya and K. Sanbongi: Preprint of Int. Iron and Steel Congress, Chicago, (1978).
30) O. Haida, T. Emi, T. Shiraishi, A. Fujiwara and K. Sanbongi: Tetsu-to-Hagané, **64** (1973) 10, p. 1538